

Resolving the structure-energy dilemma at organic-inorganic interfaces: Adsorption of benzene, thiophene and xenon over coinage metal surfaces

Santosh Adhikari,^{1, a)} Niraj K. Nepal,¹ Hong Tang,¹ and Adrienn Ruzsinszky¹
Department of Physics, Temple University, Philadelphia, PA-19122, USA

(Dated: 5 January 2021)

Semilocal (SL) density functional approximations (DFAs) are widely applied but have limitations due to their inability to incorporate long-range van der Waals (vdW) interaction. Non-local functionals (vdW-DF, VV10, rVV10) or empirical methods (DFT+D, DFT+vdW, DFT+MBD) are used with SL-DFAs to account for such missing interaction. The physisorption of a molecule on the surface of the coinage metals (Cu, Ag, and Au) is a typical example of systems where vdW interaction is significant. However, it is difficult to find a general method that reasonably describes both adsorption energy and geometry of even the simple prototypes of cyclic and heterocyclic aromatic molecules like benzene (C₆H₆) and thiophene (C₄H₄S) respectively, with reasonable accuracy. In this work, we present an alternative scheme based on Zaremba-Kohn theory, called DFT+vdW-dZK. We show that, unlike other popular methods, DFT+vdW-dZK and particularly SCAN+vdW-dZK gives an accurate description of the physisorption of a rare-gas atom (Xe) and two small albeit diverse prototype organic molecules on the (111) surfaces of the coinage metals.

I. INTRODUCTION

The interface between an organic molecule and a metallic surface plays a significant role in diverse fields such as optoelectronics, catalysis, sensors, and surface-photochemistry.¹⁻⁵ Benzene (C₆H₆) and thiophene (C₄H₄S) are respectively the most studied⁶⁻⁸ prototypes of the cyclic and the heterocyclic aromatic molecules to model⁹⁻¹² such an interface. There are experimental techniques like temperature-programmed desorption (TPD), normal incidence X-ray standing wavefield absorption (NIXSW), and near-edge X-ray absorption fine structure spectroscopy (NEXAFS) to help determine the adsorption energy and geometry at the interface. However, experimental results are affected by surface defects, monolayer formation, the orientation of the adsorbate, etc., and require analysis from several experiments to be put together for the full picture.³ These difficulties motivate the need for computational tools that are able to mimic the mechanism that requires a delicate balance between the short- and long-range interactions (mainly van der Waals (vdW) effect).¹³⁻¹⁶ Being a nonlocal effect, the latter poses a tough challenge for theoretical methods.

Wave-function based approximations like coupled-cluster (CC) can account for the vdW effect with greater accuracy but are computationally out of reach for such interface models. Alternatively, density functional theory (DFT)^{17,18} provides a framework for electronic structure calculations in diverse fields¹⁹ through different rungs of approximations illustrated by the Jacobs ladder of Perdew.²⁰ High-level approximations like the random phase approximations (RPA) within this framework are nearly exact for the long-range vdW effect.²¹ But, despite the increased computational power and efficient implementation,²² RPA is unable to handle supercell calculations involving a relatively large numbers of atoms. DFT can accommodate these calculations at the semilocal (SL) level, but the required long-range correlation effects are missing here.

Therefore, SL density functional approximations (DFAs) are often combined with a nonlocal correlation functional²³⁻²⁶ or an empirical method^{11,12,27-34} that relies on input polarizabilities, mostly through some adjustable parameters to include the vdW effects. These adjustable parameters guide the delicate balance between the short-range interactions captured by DFAs (base functionals) and the long-range interactions that the correction methods provide.³⁵

GGAs (generalized gradient approximations) are superior to LDA for aromatic systems³⁶ and hence are the natural choices as base functionals. PBE³⁷ and its revised versions³⁸⁻⁴⁰ and the Becke functionals⁴¹⁻⁴³ are some successful^{9,10,44-49} base functionals at the GGA level. Despite being widely used, GGAs by themselves are unable to capture vdW interaction beyond the short-range while the SCAN⁵⁰ metaGGA does. SCAN, by construction, can recognize different bonding environments. There are a few instances like formation energies of weakly bound intermetallics,⁵¹⁻⁵³ and prediction of magnetic properties of transition metals,⁵⁴ where SCAN is not up to the mark, but it has been mostly successful for diversely bonded systems.⁵⁵⁻⁵⁹ Recently, SCAN was revised (revSCAN⁶⁰) by diminishing its intermediate-ranged vdW interaction, leading to better interaction energies of molecules of the S22 dataset when combined with VV10²⁵ than SCAN+VV10. However, when combined with rVV10,²⁶ SCAN is remarkably accurate for molecular complexes, solids, and layered materials.⁶¹ Both VV10 and rVV10 are nonlocal correlation functionals like vdW-DFs,^{23,24} paired with the base functional as

$$E_{xc} = E_{xc}^{DFA} + E_c^{nl}, \quad (1)$$

where E_{xc}^{DFA} is the total exchange-correlation energy computed from the base functional, while E_c^{nl} is the nonlocal electron-correlation energy. These schemes bridge the nonlocal correlation functionals to the semilocal functional through a few parameters and depend only on the electron density as input.

There is an alternative way to include the vdW interaction through empirical methods where the base functional is often combined as

$$E_{tot} = E_{DFA} + E_{vdW}, \quad (2)$$

^{a)}Electronic mail: tuf60388@temple.edu.

where E_{DFA} is the total energy computed from the base functional while E_{vdW} is the contribution to the total energy due to vdW interaction. Methods like DFT+D^{62,63} model the latter part as a C_6 coefficient-based pairwise additive interaction. The C_6 coefficients utilized here are unable to adjust to the chemical environment (system) and neglect the many-body dispersion effects. But methods like DFT+D3,^{64,65} XDM²⁷⁻²⁹(exchange-hole dipole moment), and DFT+vdW¹¹ incorporate the information of the system through different ways.³⁵

In our present assessment, we are investigating the adsorption of benzene, thiophene, and xenon over the (111) surfaces of the coinage metals. Several past studies have suggested the physisorption of these systems on such coinage metal surfaces. However, it is difficult for even the improved empirical functionals to model such an interface due to the screening of molecule-surface interaction.

We present in the Methodology section a brief introduction of the recently proposed model⁶⁶ based on Zaremba-Kohn's second-order perturbation theory designed for modeling the physisorption of a particle over the surface that naturally incorporates the screening effects. This model yields RPA quality results for the physisorption of graphene over metallic surfaces^{66,67} and semiconducting layered materials. In our previous work,⁴⁹ we showed that this method outperforms all other semilocal functionals paired with rVV10 for adsorption of thiophene on coinage metal surfaces. We note that the model DFT+vdW³⁴ is based on Lifshitz-Zaremba-Kohn's theory, too. However, that model includes the screening effects through the C_6 instead of C_3 coefficients and has no high order terms, such as quadrupolar C_5 .

II. METHODOLOGY

A recently introduced model⁶⁶ based on the damped Zaremba-Kohn⁶⁸⁻⁷⁰ (dZK) second-order perturbation theory addresses the vdW interaction for physisorption of graphene over a metallic surface. In this model, the asymptotic form of the vdW interaction between a particle and a clean surface accounts^{71,72} for vdW energy as

$$E_{vdW} = \left[-\frac{C_3}{(z-z_0)^3} - \frac{C_5}{(z-z_0)^5} \right] f_d. \quad (3)$$

In Eq. (3), z_0 is the reference plane position and $z = d - c/2$, where d is the distance between the particle and the surface and $c = a/\sqrt{h^2 + k^2 + l^2}$ with h , k , and l being the Miller indices of the surface of transition metal having lattice constant a . Here the C_3 coefficient describes the dielectric response of the bulk solids to the instantaneous dipole moments of the particle, and the C_5 coefficient gives the fluctuating quadrupole (C_5^q), nonlocal (C_5^{nl}) and diffuse (C_5^d) contributions of the particle (see Tao *et al.*⁶⁶ and references therein for more details). In the dZK model, the dynamic dielectric response from the substrates includes the screening effects. The C_3 and C_5^q terms here are portrayed as a kind of local form, in which the sub-

strate response is approximated in terms of an average dielectric function, computed at wave vector $q = 0$. The C_5^d and C_5^{nl} terms are derived from the hydrodynamic model at electrostatic limits, and are dipolar contributions to the term $\sim 1/(z-z_0)^5$. The wave vector ($q \neq 0$) dependence is included in the derivations of C_5^d and C_5^{nl} .^{71,72} Those terms include effects of a nonlocal dielectric function. This model relies on the highly accurate static polarizabilities from experiment^{73,74} or from high-level calculations.⁷⁵⁻⁷⁷ The damping factor for Eq. (3) is

$$f_d = \frac{x^5}{(1 + gx^2 + hx^4 + x^{10})^{\frac{1}{2}}} \quad (4)$$

where, $x = \frac{z-z_0}{b} > 0$, $g = \frac{2b^2C_3}{C_5}$ and $h = \frac{10b^4C_3^2}{C_5^2}$. The cutoff parameter b , which is our only fit parameter, is determined by minimizing the mean absolute error (MAE) between calculated and RPA binding energies of graphene over the transition metal surfaces.^{66,67} Based on previous work,^{49,67} we used $b=3.3$ Bohr for PBE+vdW-dZK. Here we are using $b=4.1$ Bohr for SCAN+vdW-dZK. Instead of taking the static dipole polarizability of the molecule, we base our C_3 coefficients on the "renormalized atom" approach.⁶⁷ The best polarizability for a particular atom (H, C, or S) in thiophene or (H or C) in benzene is then renormalized as

$$\alpha_{(renormalized_atom)} = \frac{\alpha_{(free_atom)}}{4\alpha_{(C)} + 4\alpha_{(H)} + \alpha_{(S)}} \alpha_{(thiophene)} \quad (5)$$

for thiophene, and

$$\alpha_{(renormalized_atom)} = \frac{\alpha_{(free_atom)}}{6\alpha_{(C)} + 6\alpha_{(H)}} \alpha_{(benzene)} \quad (6)$$

for benzene.

With the static polarizabilities, we can find the separate C_3 and C_5 coefficients for each of the elements in the molecule (see Tables (S1-S3) in Supplementary Materials for the computed C_3 and C_5 coefficients for xenon, and renormalized atoms in benzene and thiophene along with the reference plane positions (Z_0)). The formula of renormalization we are using is for a "particle" interacting with a metal surface. Despite that both benzene and thiophene are relatively small molecules, we can not treat them as particles. Treating them as particles would overestimate C_5 significantly.⁴⁹ Thus we treat benzene and thiophene as a collection of renormalized atoms.

III. COMPUTATIONAL DETAILS

All the DFT calculations performed utilized the projector augmented wave (PAW) formalism implemented in the Vienna ab initio simulation package (VASP) code. Geometry relaxations of the bulk structures of silver, gold, and copper using different XC functionals yielded the respective lattice constants (see Table S4 in Supplementary Materials for calculated lattice constants compared to the experimental zero-point phonon corrected lattice constants.⁷⁸) Since a

study by Carter *et al.*⁷⁹ showed a non-negligible interaction of the adsorbate-molecule with its periodic image for a relatively smaller (3×3) supercell, we opted to build a (4×4) supercell of 111 surfaces in the atomic simulation environment (ASE)^{80,81} using the optimized lattice constants. The supercell has a five-atomic-layer thickness. A vacuum of 12 Å was added along the z-direction to prevent the interactions due to the periodic images. The positions of the atoms on the bottom three layers were fixed during the relaxation to reduce the computational cost. Benzene and thiophene constructed using the reference C-S, C-C, and C-H bond lengths^{82,83} were allowed to relax in the slab whose size was identical to that of the surface on which the adsorption occurred. Initially, both thiophene and benzene were placed in a parallel orientation 3Å above the top metal layer and were allowed to relax on the high-symmetry sites (fcc, hcp, ontop, and bridge).^{80,81} Those sites were defined using the center of mass and the azimuthal angle of the molecule as proposed by Liu *et al.*⁴⁶ For example, hcp-45 indicates the center of mass of thiophene adsorbed at hcp site with a symmetry axis rotated by 45° from the direction of metal rows. The surface, the molecule, and the molecule-surface system were all separately relaxed. We utilized a similar procedure for the adsorption of xenon (Xe) over the (111) surfaces of Ag and Cu, as well, except that Xe being an atom was just placed above the aforementioned high-symmetry sites without rotation. We used the VASP recommended PAW pseudopotentials for all the calculations. While we utilized a plane-wave cutoff of 650 eV, the smearing parameter ($k_B T$) of 0.1 eV was used following the first order Methfessel-Paxton scheme. We used $4 \times 4 \times 1$ and $20 \times 20 \times 20$ Monkhorst-Pack meshes for the Brillouin zone sampling of the surface and the bulk, respectively. Since both adsorption energies and equilibrium distances depend on the adsorption-site, we utilized all major high symmetry sites for PBE+vdW-dZK and SCAN+vdW-dZK calculations. However, we only used the most stable site (hcp-30 for benzene and fcc-45 for thiophene) for the computation from other methods. We calculated the adsorption energy by subtracting the energy of the surface and molecule from the surface-molecule system.

$$E_{ad} = E_{surf+mol} - E_{surf} - E_{mol} \quad (7)$$

We adopted similar procedure for calculating the adsorption energy of Xe over the metallic surfaces.

For DFT+vdW-dZK calculations, we computed the C_3 , C_5^q , C_5^{nl} , and z_0 terms using Eqs (2-4) from the work of Tao *et al.*⁶⁶ Since the diffuse part (C_5^d) is small compared to the nonlocal and quadrupole parts,^{66,72} we compute C_5 as a sum of the C_5^{nl} and C_5^q terms (see Tables (S1-S3) in Supplementary Materials for the computed C_3 and C_5 coefficients for xenon, and renormalized atoms in benzene and thiophene along with the reference plane positions (z_0)). All the parameters required for the transition metals were taken from the previous work.^{66,67} We utilized the experimental static dipole polarizabilities reported in the NIST⁷⁴ database for all atoms and molecules studied in our work. Finally, we computed the total adsorption energy at each distance by adding the adsorption energy from DFT calculations and the corresponding correction obtained from vdW-dZK model (Eq (3)), following the binding-curve

approach as in Fig. 1 of Tang *et al.*⁶⁷ (see Figures (S1-S8) in Supplementary Materials for the computed adsorption energies for benzene, thiophene and Xe over the (111) surfaces of coinage metals using PBE+vdW-dZK and SCAN+vdW-dZK).

IV. RESULTS AND DISCUSSION

We have assessed the adsorption energies, the vertical adsorption distances, and the tilt angles of benzene and thiophene placed over the (111) surfaces of Cu, Ag, and Au (coinage metals) using the scheme based on the physisorption model (vdW-dZK)⁶⁶ following Zaremba-Kohn theory. Currently, this scheme⁶⁶ has been implemented to PBE³⁷ (PBE+vdW-dZK^{49,67}) and very recently the modified⁸⁴ form of that scheme to SCAN metaGGA. In this work we are implementing the original scheme⁶⁶ (without any modifications), to SCAN⁵⁰ (SCAN+vdW-dZK). For comparative purposes, we also paired the semi-local functionals with the non-local functional (rVV10²⁶) or the D3⁶⁵ method. The common goal of all these methods is to capture the van der Waals (vdW) interaction that is very relevant for the adsorption process but is missing in the bare semi-local functionals. We utilized the parameters of Peng *et al.*⁶¹ based on fitting to binding energy curve of argon-dimer obtained from CCSD(T) calculations, to pair rVV10 with SCAN. In our previous work,⁴⁹ we followed the same approach to determine the parameters required to combine rVV10 with PBE, PBEsol, and revSCAN. Finally, the parameters obtained from Brandenburg *et al.*⁸⁵ were utilized to combine SCAN with D3 (SCAN+D3).

A. Benzene over Cu(111), Ag(111) and Au(111)

We utilized eight different high symmetry sites for the adsorption of benzene over the (111) surfaces of Cu, Ag, and Au, as displayed in Fig 1. Our calculations with PBE+vdW-dZK and SCAN+vdW-dZK, in agreement with Liu *et al.*,⁴⁶ show a weak dependence of adsorption energy on the site as the maximum energy difference between them is just 0.05 eV. In agreement with past studies,^{46,47,61,86} these methods, irrespective of the substrate metals, predict the hollow site (hcp-30) as the most stable site of adsorption. For better comparison, we focused on the most stable site (hcp-30) for all other methods utilized in our work.

In agreement with the experiments,⁸⁷⁻⁸⁹ all the methods discussed here including PBE+vdW-dZK and SCAN+vdW-dZK predict benzene to adsorb flat (parallel) to the metal surface without any noticeable tilting.

Table I displays the adsorption energy of benzene over the (111) surface of different metal substrates at the most stable site of adsorption. The experimental adsorption energies reported are acquired from the analysis of the data obtained from the temperature-programmed desorption (TPD) measurements. The most commonly used technique is the Redhead analysis,⁹⁰ which treats desorption temperature to be independent of the coverage and uses a frequency parame-

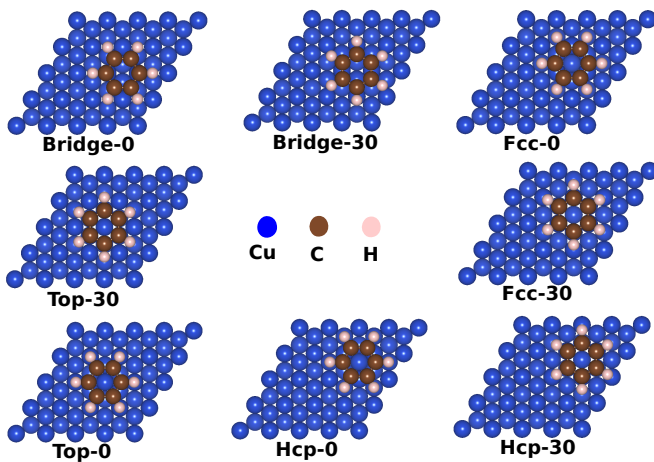


FIG. 1: The figure shows the high symmetry sites⁸⁰ utilized for the initial adsorption of a benzene molecule over the (111) surface of Copper.

ter often guessed over a range of values ($[10^{12} - 10^{15}] \text{ s}^{-1}$). However, the TPD measurements display a correlation between the coverage and the desorption temperature, questioning the Redhead's analysis. A recent experimental study⁴⁵ utilizes the so-called complete analysis,⁹¹ where the frequency factors are determined uniquely for a given coverage. This experiment⁴⁵ benchmarks the adsorption energy for benzene adsorbed (within an error bar of 0.05 eV) on the (111) surface of the coinage metals, enabling one to test the accuracy of the theoretical methods.

PBE largely underestimates the adsorption energies due

TABLE I: Adsorption energy (in eV) of benzene (C_6H_6) when placed on the most stable site (hcp-30) over the (111) surfaces of coinage metals using the different methods. The results from various previous studies are also reported here for comparison.

	$\text{C}_6\text{H}_6/\text{Cu}(111)$	$\text{C}_6\text{H}_6/\text{Ag}(111)$	$\text{C}_6\text{H}_6/\text{Au}(111)$
PBE	-0.06	-0.06	-0.06
PBE+rVV10	-0.58	-0.54	-0.60
PBE+D3	-1.00	-0.86	-0.93
PBE+vdW-dZK	-0.56	-0.60	-0.67
PBE+vdW ⁹²	-1.07	-0.87	-0.84
PBE+vdW ^{surf93}	-0.86	-0.75	-0.74
PBE+MBD ⁴⁵	-0.63	-0.57	-0.56
PBE+XDM ¹⁰	-0.54	-0.58	-0.61
B86bPBE+XDM ¹⁰	-0.59	-0.68	-0.64
optPBE+vdw-DF ⁴⁴	-0.68	-0.71	-0.71
SCAN	-0.43	-0.40	-0.42
SCAN+rVV10	-0.78	-0.75	-0.80
SCAN+D3	-0.93	-0.81	-0.86
SCAN+vdW-dZK	-0.63	-0.60	-0.65
revSCAN+rVV10	-1.11	-0.93	-1.03
HSE+MBD ⁴⁵	-0.78	-0.68	-0.67
Expt ⁴⁵	-0.68 ± 0.04	-0.63 ± 0.05	-0.71 ± 0.03

to its inability to capture the vdW interaction beyond short-range. SCAN by design can incorporate some intermediate-range interaction, but as evident in our calculations, these are still not sufficient to fully account for the missing long-range vdW interaction. Non local correlation functionals like rVV10,²⁶ VV10²⁵ and vdW-DFs^{23,24} can often be paired with semilocal (SL) density functional approximations (DFA) to incorporate such missing interaction. However, our work suggests that the rVV10-based methods are inconsistent due to their over-flexibility in pairing with the base functionals. We will elaborate more on this puzzle in the later sections. There are alternative empirical ways to include vdW interactions such as the popular method DFT+D3,^{64,65} known for identifying the local chemical environment through improved C_6 coefficients. These methods, in comparison to their predecessors,^{62,63} are much accurate for interaction energies of molecular systems like the S22 data set, rare-gas dimers, etc. But in agreement with the previous work,⁹ we found over-estimated adsorption energies with these methods. Since the effect of surface metal atoms screening the molecule-surface interaction is ignored even in these improved C_6 coefficients, it could be the major reason behind the poor performance of these methods for our systems. In the DFT+vdW¹¹ method, the C_6 coefficients along with the vdW radii are determined using the electron density obtained from the base functionals, and are independent of these underlying base functionals. However, like DFT+D, this method also lacks screening effects leading to significantly overestimated⁹² adsorption energies. The method DFT+vdW^{surf34} was introduced to include the screening effects in DFT+vdW following Lifshitz-Zaremba-Kohn^{68,69} theory. Here, the screening effects were included using modified C_6 coefficients rather than explicitly using the C_3 coefficients pertinent for particle-slab interaction. PBE+vdW^{surf} predicted better⁹³ adsorption energies compared to PBE+vdW⁹² but still the overestimation was noticeable. Another approximation, the DFT+MBD,¹² was introduced to incorporate the screening effects in DFT+vdW. This method reported better adsorption energies⁴⁵ when combined with a hybrid functional (HSE). However, using a hybrid base functional is computationally demanding. Similarly the method PBE+XDM,¹⁰ based on the exchange-hole dipole moment,^{27,29} reports slightly underestimated adsorption energies. In Table I, we show the results from other important methods from previous studies,^{10,45,92,93} as well.

Among all reported methods, SCAN+vdW-dZK stands out. The adsorption energies of benzene over different metal substrates predicted from this method lie close to the error bars of the reported reference values. In Fig. 2 we show the absolute deviation of the adsorption energies calculated using different methods in our work from the reported experimental values. Despite slightly underbinding benzene on a copper surface, PBE+vdW-dZK lies closest to the reference values for the other two metal surfaces (see Figures (S1-S3) in the Supplementary Materials for the details on PBE+vdW-dZK and SCAN+vdW-dZK calculations). The adsorption energies predicted from both vdW-dZK based methods are close to each other as was also the case for graphene over layered materials,⁸⁴ which shows the consistency of these meth-

ods for adsorption energies. Recently, Chowdhury *et al.*⁹⁴ have extended the vdW-dZK model to address the adsorption of molecules on carbon nanotubes, which have curved cylindrical surfaces. The binding energies calculated from PBE+vdW-dZK and SCAN+vdW-dZK are very close to each other. It further confirms the consistency of the vdW-dZK model.

Finally, based on the molecular orbital density of states

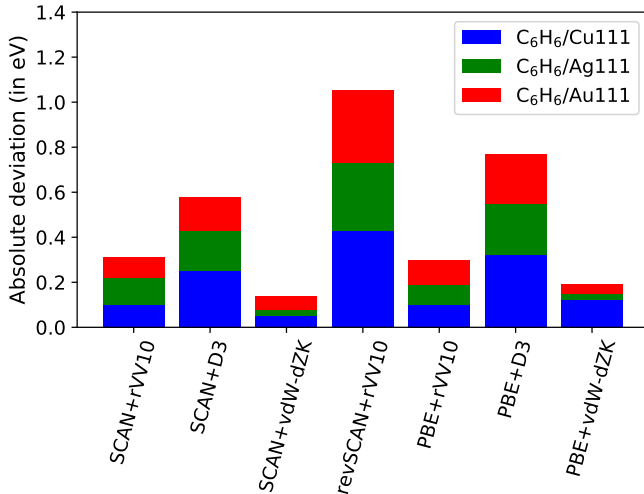


FIG. 2: Figure shows the absolute deviation between adsorption energies (in eV) of benzene (C_6H_6) on the (111) surfaces of Cu, Ag, and Au calculated using various methods studied in our work and the experimental value obtained from the complete analysis.⁹¹ We note that the uncertainties (not shown in figure) in the experimental values⁴⁵ are ± 0.04 eV, ± 0.05 eV, and ± 0.03 eV for C_6H_6 on the (111) surfaces of Cu, Ag, and Au respectively.

(MODOS) analysis by Jiang *et al.*,⁹³ the d-band center for benzene on Ag(111) lies farther away from the Fermi-level than for benzene on Au(111) surface. From the perspective of d-band center theory,⁹⁵⁻⁹⁷ this means that Au(111) should be more reactive than Ag(111) for benzene. The experimental adsorption energies obtained from the so-called complete analysis of TPD measurements support this prediction of d-band center theory too. In this regard, SCAN+vdW-dZK and PBE+vdW-dZK both appear to be qualitatively accurate as well. Though the adsorption energies predicted from methods like PBE+MBD, HSE+MBD, and optPBE+vdW-DF were reasonable, all those methods predict almost equal adsorption energies of benzene on Ag(111) and Au(111) against the trend predicted by the experiment and the d-band center theory.

Although adsorption energies over different metallic surfaces are close to each other, Reckien *et al.*⁹ argue that the vertical adsorption distances are similar for Ag(111) and Au(111), while relatively shorter for Cu(111). This ordering of adsorption distances is consistent with the similar vdW radii of Ag and Au, both being larger than that of Cu. To the best of our knowledge, we have experimental data for ad-

TABLE II: Adsorption distance (in Å) of the molecule benzene (C_6H_6) when placed on the most stable site (hcp-30) over the (111) surfaces of the coinage metals using different methods. Adsorption distance from various previous studies is also reported here for comparison.

	$C_6H_6/Cu(111)$	$C_6H_6/Ag(111)$	$C_6H_6/Au(111)$
PBE	3.40	3.44	3.42
PBE+rVV10	3.01	3.02	3.01
PBE+D3	2.95	2.97	2.97
PBE+vdW-dZK	3.13	3.23	3.22
PBE+vdW ⁹²	3.04	3.14	3.21
PBE+vdW ^{surf} ⁹³	2.83	2.97	3.05
B86bPBE+XDM ¹⁰	2.71	3.03	3.15
optPBE+vdw-DF ⁴⁴	3.14	3.23	3.21
SCAN	3.01	3.10	3.18
SCAN+rVV10	2.95	2.98	3.01
SCAN+D3	2.90	3.00	2.99
SCAN+vdW-dZK	2.85	3.02	3.06
revSCAN+rVV10	2.66	2.93	2.95
Expt ⁹⁸	-	3.04 ± 0.02	-

sorption distance available⁹⁸ only for benzene over Ag(111) based on the normal-incidence x-ray standing wave (NIXSW) measurements, as shown in Table II. Though methods like SCAN+rVV10, PBE+D3, and PBE+rVV10 predict adsorption distances for benzene over Ag(111) closer to the experimental values, they predict similar adsorption distance for different metallic surfaces. SCAN, revSCAN+rVV10, and PBE+vdW-dZK get that order right but, they are quantitatively not close enough to the experimental values. Getting the adsorption distances, orientations, and energies right are challenges even for most vdW-corrected density functionals as they require a delicate balance between short- and long-range correlations. The popular method optPBE+vdW-DF⁴⁴ yields the adsorption energies very close to the experimental values but predicts longer adsorption distances. However, methods like SCAN+D3⁶⁵ predict adsorption distances within the error bar of experimental value, yet overestimate the adsorption energies. Very few methods like B86bPBE+XDM,¹⁰ PBE+vdW^{surf},^{45,93} and PBE+MBD^{45,93} give a reasonable description of the aforementioned challenges. The orientations and adsorption distances of benzene over different metallic surfaces predicted by some of the better-performing methods in our work are as shown in Fig. 3. PBE+vdW-dZK is not as impressive for adsorption distances as it was for adsorption energies, but SCAN+vdW-dZK stands out as the best overall performer. Apart from predicting the correct adsorption sites and orientations of the adsorbate molecule, SCAN+vdW-dZK yields the adsorption energies and distances within the narrow error bar of the available experimental values.

B. Thiophene over Cu(111), Ag(111) and Au(111)

In our previous work,⁴⁹ we had demonstrated how the combination of non-local functional rVV10 combined with metaGGAs failed to deliver for adsorption of the polar

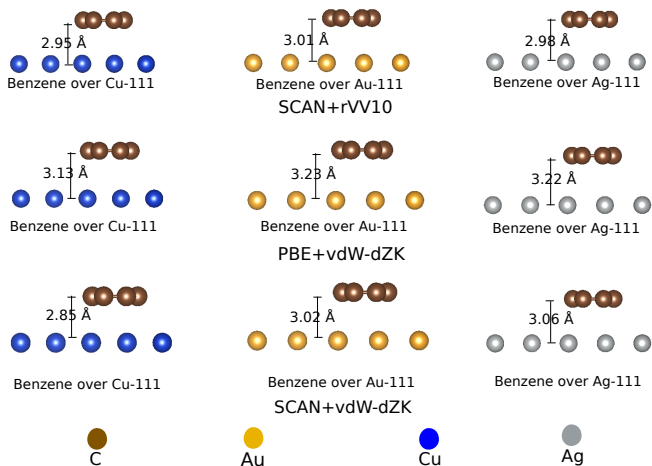


FIG. 3: The figure shows the adsorption distance of benzene over the (111) surfaces of Cu, Ag, and Au when placed at the most stable site (hcp-30). For convenience, only the results of the three better performers, namely PBE+vdW-dZK, SCAN+vdW-dZK, and SCAN+rVV10, are displayed.

molecule thiophene over the (111) surfaces of the coinage metals. We also showed how PBE+vdW-dZK was able to predict adsorption energies, orientation, and distances better than many studied and existing methods. However, in the previous section, we showed that the PBE+vdW-dZK predicted adsorption energies of benzene over coinage metals reasonably well but yielded longer adsorption distances, where SCAN+vdW-dZK was reasonable in both areas. Here we compare the performance of SCAN+vdW-dZK for thiophene over the (111) surfaces of coinage metals.

Experiments⁹⁹⁻¹⁰¹ predict the ontop position of the sulfur atom in the thiophene as the most stable site of adsorption. This site is close to the fcc-45⁸⁰ site of the center of the aromatic ring of the thiophene. Based on the given coverage, SCAN+vdW-dZK, in agreement to PBE+vdW-dZK, SCAN+rVV10, revSCAN+rVV10, PBE+rVV10, PBEsol+rVV10, predicts this fcc-45 site as the most stable site of adsorption.

While experiments^{100,102,103} demonstrate thiophene to lie flat over the (111) surfaces of Ag and Au, strong coverage dependent tilting is found⁹⁹ over the Cu(111) surface increasing from an angle $12^\circ \pm 2^\circ$ to $25^\circ \pm 4^\circ$, when the coverage varies from 0.03 ML to 0.1 ML. Most of the theoretical studies^{10,49,104} predict thiophene to lie flat even over the Cu(111) surface. SCAN+vdW-dZK, in agreement with the experiments, predicts the flat orientation of thiophene over Ag(111) and Au(111). However, the predicted tilting angle of 7° over Cu(111) is slightly less than the tilt angles observed for 0.03 ML coverage. Similar tilting was predicted by PBE+vdW^{surf}.¹⁰⁵ Though the tilting angle predicted by PBE+vdW-dZK⁴⁹ is close to the values demonstrated by the experiment, Maurer *et al.*,¹⁰⁵ argue that the tilting angles predicted by experiment at finite temperature is larger due to the anharmonicity of the adsorbate-substrate bond.

Table III displays the sulfur-substrate distance (in Å) and

TABLE III: substrate-sulfur distance (in Å) and adsorption energy (in eV) of thiophene placed on the most stable site (fcc-45) over the (111) surfaces of the coinage metals using different methods.

	C ₄ H ₄ S/Cu(111)		C ₄ H ₄ S/Ag(111)		C ₄ H ₄ S/Au(111)	
	d(Cu-S)	E _{ad}	d(Ag-S)	E _{ad}	d(Au-S)	E _{ad}
PBE+rVV10 ⁴⁹	2.88	-0.61	3.00	-0.55	2.98	-0.63
PBE+vdW ^{surf} ¹⁰⁵	2.78	-0.82	3.17	-0.72	2.95	-0.77
PBE+D2 ¹⁰⁴	2.40	-0.81	-	-	2.75	-1.24
PBE+vdW-dZK ⁴⁹	2.57	-0.60	3.16	-0.50	3.23	-0.56
B86bPBE+XDM ¹⁰	2.99	-0.62	3.04	-0.67	2.99	-0.66
PBEsol+rVV10 ⁴⁹	2.19	-1.22	2.68	-0.93	2.59	-1.06
SCAN+vdW-dZK	2.66	-0.69	3.00	-0.62	2.98	-0.69
Expt	2.62±0.03 ¹⁰⁶		-0.66 ⁹⁹		-0.52 ¹⁰³	

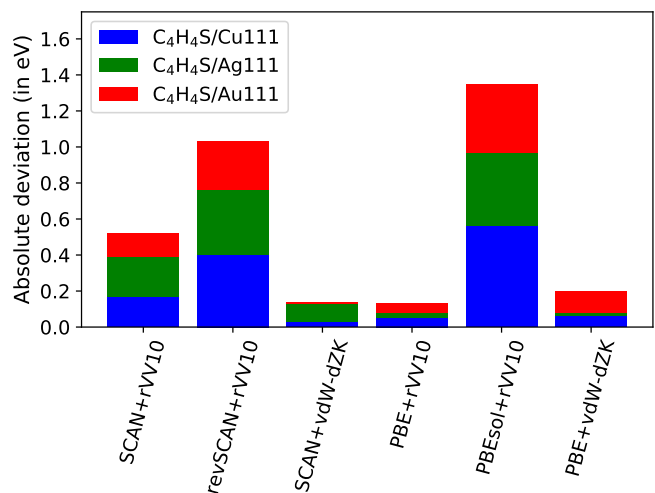


FIG. 4: Figure shows the absolute deviation between adsorption energies (in eV) of thiophene (C₄H₄S) on the (111) surfaces of Cu, Ag, and Au calculated using various methods studied in our work and the experimental value^{99,103,107} obtained using the Redhead Analysis.⁹⁰

the adsorption energy (E_{ad}) [in eV] of thiophene over different substrate metals. The experimental adsorption energies are obtained from the Redhead analysis⁹⁰ of the TPD measurements^{99,103,107} using 10^{13} s^{-1} as the frequency parameter. We note that for a given TPD measurement, the choice of frequency parameter from 10^{12} s^{-1} to 10^{15} s^{-1} can lead to differences up to 0.2 eV. But, since thiophene is a small molecule, our choice of frequency parameter, we believe, is a reasonable one. We also note that this frequency parameter is consistent with the choice made by Christian *et al.*¹⁰ for Redhead analysis on similar work. Unfortunately, we have the substrate-sulfur distance available only for thiophene on Cu(111) based on S K-edge X-ray-absorption fine structure measurements.^{106,108} In Fig. 4, we display the absolute deviation of the adsorption energies predicted by various methods in our work from the experimental values^{99,103,107} obtained using the Redhead analysis.⁹⁰ While popular methods like

PBE+D2¹⁰⁴ overestimate E_{ad} and predict shorter distances, methods like B86bPBE+XDM¹⁰ and PBE+rVV10⁴⁹ predict reasonable adsorption energies but yield longer distances. PBE+vdW-dZK predicts the substrate-sulfur distance for thiophene over Cu(111) closer to the experimental value, but it slightly underestimates the adsorption energies. SCAN+vdW-dZK, though it slightly overestimates the adsorption energy of thiophene on Ag(111), is the best overall performer (see Figures S4-S6 in the Supplementary Materials for the details of SCAN+vdW-dZK calculations). Fig. 5 displays the orientation and sulfur-adsorbate distance of thiophene over the (111) surfaces of coinage metals for the three better-performing methods.

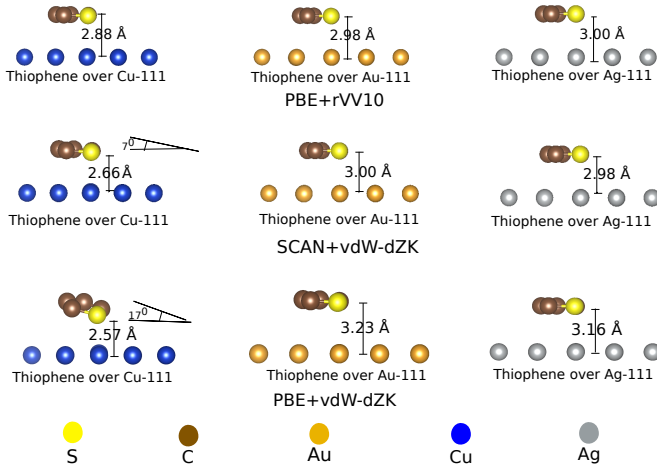


FIG. 5: Figure shows the adsorption distance and tilt angle of thiophene over the (111) surfaces of Cu, Ag, and Au placed at the most stable site of adsorption (fcc-45). For convenience, results of the three better performers namely PBE+vdW-dZK, SCAN+vdW-dZK, and PBE+rVV10, are shown.

C. Xenon (Xe) over Cu(111) and Ag(111)

As a further test of vdW-dZK model, we assessed the adsorption energy and distance of Xe over the (111) surfaces of Cu and Ag. The binding of Xe with the substrate metal surfaces is a typical physisorption case dominated by vdW interaction. We compare the results from the vdW-dZK methods to the adsorption energies and distances reported by other existing vdW-corrected methods in Table IV. The experimental values tabulated here are from the so-called best estimate,¹⁰⁹ and the review work of Diehl *et al.*¹¹⁰ (see the references therein for more details on experimental results). Although all reported methods agree to the ontop site as the most stable adsorption-site, they predict significantly different adsorption energies and distances. While SCAN without any vdW correction gives the best estimate of the adsorption distances, it significantly underestimates the adsorption energies. In contrast, the non-local correlation functional vdW-

TABLE IV: Xe-substrate distance (in Å) and adsorption energy (in meV) of Xe placed on the most stable site (ontop) over Ag(111) and Cu(111).

	Xe/Cu(111)		Xe/Ag(111)	
	E_{ad}	$d(\text{Xe-Cu})$	E_{ad}	$d(\text{Xe-Ag})$
PBE	-21	4.25	-21	4.27
PBE+vdW ¹¹¹	-335	3.48	-244	3.60
PBE+vdW ^{surf} ¹¹¹	-248	3.46	-237	3.57
PBE+vdW-dZK	-252	3.29	-275	3.37
PBEsol+rVV10s ⁴⁸	-165	3.5	-186	3.4
vdW-DF ¹¹²	-184	3.97	-180	4.08
vdW-DF2 ¹¹²	-157	4.01	-154	4.00
SCAN	-90	3.61	-93	3.57
SCAN+vdW-dZK	-187	3.47	-197	3.49
Expt ^{109,110}	$-(183 \pm 10)$	3.60 ± 0.08	$-(211 \pm 15)$	3.60 ± 0.05

DF gives a better description of adsorption energies but yields longer adsorption distances.¹¹² Although the performance of PBE+vdW is mixed, PBE+vdW^{surf} gives a reasonable estimate of both adsorption energies and distances.¹¹¹ While PBE+vdW-dZK performs on similar lines with PBE+vdW^{surf} for the adsorption energy of Xe over Cu(111), it gives a slightly overestimated value of the adsorption energy for Xe over Ag(111). PBE+vdW-dZK predicts slightly shorter adsorption distances for Xe over both the surfaces as well. Although PBEsol+rVV10s⁴⁸ performs better than the most methods discussed here, SCAN+vdW-dZK stands out overall by predicting both adsorption energies and equilibrium distances closer to the error bars of the available experimental values^{109,110} (see Figures S7 and S8 in the Supplementary Materials for the details on PBE+vdW-dZK and SCAN+vdW-dZK calculations).

D. Performance of the rVV10-based methods

In our present study, we utilized a nonlocal correlation functional rVV10²⁶ paired with PBE, PBEsol, SCAN, and revSCAN to include the long-range vdW effects required for the accurate description of the organic molecule adsorbed over the metallic surfaces. We noticed a strong discrepancy in the description of the molecule-metal system between different rVV10 based methods. While PBE+rVV10 slightly underestimates the adsorption energies for benzene, it gives a reasonable description in the case of thiophene. SCAN+rVV10 overestimates in the case of adsorption of both molecules. Some recent studies^{59,84} suggest SCAN+rVV10 to be overestimating in general. When combined with revSCAN,⁶⁰ rVV10 is significantly overestimating the adsorption energies of those molecules over the metallic surfaces. Although revSCAN⁶⁰ was designed to remove the intermediate-range interactions of SCAN, when paired with rVV10, it proved to be over-correcting. PBEsol+rVV10 yields almost double the adsorption energies of thiophene over metallic surfaces compared to PBE+rVV10.⁴⁹ But, rVV10 is not the only nonlocal functional to demonstrate such strong dependence on the base functional to which it combines. A noticeable dependence on

base functionals was reported for nonlocal correlation functionals such as vdW-DFs,^{23,24} as well. When the revPBE³⁸ base functional proposed for vdW-DF²³ was replaced by the revised version¹¹³ of PW86¹¹⁴ for vdW-DF2,²⁴ it yielded better accuracy for molecular complexes. While both these base functionals⁴⁴ underestimated the adsorption energies for benzene on coinage metals, the pairing with less repulsive base functionals⁴⁰ like optPBE and optB88 gave a better description.

rVV10, unlike vdW-DFs, is much more flexible to pair with the base functional and does so with a set of parameters, namely ‘b’ and ‘C.’ The former controls the short-range damping while the latter controls the accuracy of the C_6 coefficient at large separation. Most studies regarding parameterization^{26,47,49,61} of rVV10 keep the value of ‘C’ equal to 0.0093 fixed as originally proposed by Vydrov *et al.*,²⁵ as changing ‘C’ does not significantly change the binding curve.⁶¹ Therefore, it is usually a single parameter ‘b’ that defines the pairing. Determination of this parameter requires fitting to well-benchmarked systems where the vdW interaction is significant, such as interaction energies of the S22 data set, the binding energy of rare-gas dimers, and interlayer binding energies of layered materials. However, we noticed a significant inconsistency in the performance of the rVV10 based methods when we determined the parameters for a particular base functional from different possible fitting methods. It is a more serious problem as this creates enough doubts over which parameterization to choose for combining rVV10 to a particular base functional for the particular problem. Fortunately for SCAN+rVV10,⁶¹ the ‘b’ parameter obtained from fitting to the binding energy of rare-gas dimers produced fewer errors for other systems as well. The ‘b’ parameter for PBE+rVV10 is 6.6 and 10.0 when fitted to the interaction energies of the S22 data set and interlayer binding energies of the layered materials, respectively.⁴⁷ However, both these values are different (b=9.7) from the parameter obtained by fitting to the argon-dimer binding energy.⁴⁹ In our previous work⁴⁹ we obtained b=9.7 for PBEsol+rVV10 using the argon dimer parameterization, which is significantly different from b=20 based on fitting to the interlayer binding energy of layered materials.⁴⁸ The latter choice of the parameter significantly underperformed for binding energies of the argon dimer compared to the former and was also unsatisfactory for interaction energies of the S22 data set compared to PBE+rVV10 (b=6.6) and SCAN+rVV10.

In Table V, we compare the adsorption energy of thiophene over the coinage metals, at the most stable site (fcc-45), from the different parameterization of rVV10 for PBE or PBEsol. We observed significant differences in the adsorption energies when different parameterizations combined rVV10 to the same base functional, illustrating the inconsistency in the performance of rVV10-based methods. The need for an improved two-parameter damping function of rVV10 is being explored by Tang, Chowdhury, and Perdew¹¹⁵, and it would hopefully solve larger parts of this problem.

TABLE V: Comparison of adsorption energies (in eV) of PBE+rVV10 and PBEsol+rVV10 based on separate parameterizations using the S22 data set, Ar₂ binding energies and interlayer binding energies of layered materials (LM) for thiophene adsorbed on the (111) surface of coinage metals.

	ref	PBE+rVV10		PBEsol+rVV10	
		Ar ₂	S22	Ar ₂	LM
Cu	-0.66 ⁹⁹	-0.61	-0.95	-1.22	-0.75
Au	-0.68 ¹⁰⁷	-0.63	-0.94	-1.06	-0.69
Ag	-0.52 ¹⁰³	-0.55	-0.82	-0.93	-0.59

V. CONCLUSION

In this work, we investigated the geometry and energetics of the adsorption of xenon and two widely studied prototype molecules, namely, benzene, and thiophene, over the (111) surface of the coinage metals using density functional theory (DFT).

Recently, the so-called complete analysis method⁹¹ was used to analyze the temperature-programmed desorption (TPD) measurement of benzene over coinage metal surfaces⁴⁵ yielding adsorption energies within an error bar of chemical accuracy (0.04 eV). Based on our results, the recently introduced model based on Zaremba-Kohn’s second-order perturbation theory (DFT+vdW-dZK) predicts the adsorption energies of benzene over metal surfaces better than any other methods reported here. In particular, SCAN+vdW-dZK stands out. Apart from yielding the correct orientation and site, this method predicts the energies and distances within the error bar of the experiment. SCAN+vdW-dZK predicts Au(111) to be more reactive than Ag(111), supporting the popular d-band center theory. SCAN+vdW-dZK is the best overall performer for xenon and thiophene over the metallic surfaces, as well. We note that due to the unavailability of the results from the complete analysis, Readhead’s analysis,⁹⁰ which is also widely used but not as accurate as the former, was utilized here to analyze the TPD measurements of thiophene adsorbed over the metallic surfaces.

Finally, through the example of thiophene adsorbed on metal surfaces, we demonstrate that the rVV10 based methods are inconsistent. They predict significantly different adsorption energies of a molecule-metal system when the same base functional pairs with rVV10 through different possible parametrizations. The current rVV10 is essentially a pairwise form in which the screening effects of metal substrates are not included explicitly in the molecule-metallic surface interactions. The vdW-dZK model incorporates such screening effects explicitly via the C_3 and C_5 nonlocal terms making the model more accurate to describe the molecule-metallic surface interactions. Although the vdW-dZK model combines with PBE or SCAN through a single parameter ‘b’, this model relies on the accurate static dipole polarizabilities as an input parameter. In our present work, we show that SCAN+vdW-dZK is slightly better than PBE+vdW-dZK on the overall performance. The adsorption distances predicted

by SCAN+vdW-dZK show better agreement with the experimental values compared to PBE+vdW-dZK. However, there are no significant differences in the adsorption energies predicted by these methods. Despite the vdW-dZK methods combining with two different functionals PBE and SCAN, it is remarkable that the adsorption energies both these methods predict are close to each other, and importantly, both close to the experimental values.

ACKNOWLEDGMENTS

S.A. and A.R. acknowledge the support of the U.S. Department of Energy, Office of Science, Office of Basic Energy Sciences, as part of the Computational Chemical Sciences Program under Award No. DE-SC0018331. H.T. acknowledges support from the DOE Office of Science, Basic Energy Sciences (BES), the U.S. Department of Energy, under Grant No. DE-SC0018194. The work of N.K.N. was supported by the National Science Foundation (NSF), under the grant number DMR-1553022. This research includes calculations carried out on HPC resources supported in part by the NSF through major research instrumentation grant number 1625061 and by the U.S. Army Research Laboratory under contract number W911NF-16-2-0189. We thank Prof. John P. Perdew for his valuable help throughout.

- ¹N. Koch, N. Ueno, and A. T. S. Wee, *The molecule-metal interface* (John Wiley & Sons, 2013).
- ²M. Oehzelt, N. Koch, and G. Heimel, "Organic semiconductor density of states controls the energy level alignment at electrode interfaces," *Nature Communications* **5**, 1–8 (2014).
- ³G. Witte and C. Wöll, "Growth of aromatic molecules on solid substrates for applications in organic electronics," *Journal of Materials Research* **19**, 1889–1916 (2004).
- ⁴"Fundamental studies of hydrodesulfurization by metal surfaces, author=Friend, Cynthia M and Chen, Donna A," *Polyhedron* **16**, 3165–3175 (1997).
- ⁵P. Gomez-Romero, "Hybrid organic–inorganic materials—in search of synergic activity," *Advanced Materials* **13**, 163–174 (2001).
- ⁶A. Takahashi, F. H. Yang, and R. T. Yang, "New sorbents for desulfurization by π -complexation: thiophene/benzene adsorption," *Industrial & Engineering Chemistry Research* **41**, 2487–2496 (2002).
- ⁷A.-L. Revelli, F. Mutelet, and J.-N. Jaubert, "Extraction of benzene or thiophene from n-heptane using ionic liquids. NMR and thermodynamic study," *The Journal of Physical Chemistry B* **114**, 4600–4608 (2010).
- ⁸S. Adhikari, B. Santra, S. Ruan, P. Bhattarai, N. K. Nepal, K. A. Jackson, and A. Ruzsinszky, "The Fermi–Löwdin self-interaction correction for ionization energies of organic molecules," *The Journal of Chemical Physics* **153**, 184303 (2020).
- ⁹W. Reckien, M. Eggers, and T. Bredow, "Theoretical study of the adsorption of benzene on coinage metals," *Beilstein Journal of Organic Chemistry* **10**, 1775–1784 (2014).
- ¹⁰M. S. Christian, A. Otero-de-la Roza, and E. R. Johnson, "Surface adsorption from the exchange-hole dipole moment dispersion model," *Journal of Chemical Theory and Computation* **12**, 3305–3315 (2016).
- ¹¹A. Tkatchenko and M. Scheffler, "Accurate molecular van der Waals interactions from ground-state electron density and free-atom reference data," *Physical Review Letters* **102**, 073005 (2009).
- ¹²A. Tkatchenko, R. A. DiStasio Jr, R. Car, and M. Scheffler, "Accurate and efficient method for many-body van der Waals interactions," *Physical Review Letters* **108**, 236402 (2012).
- ¹³A. Tkatchenko, L. Romaner, O. T. Hofmann, E. Zojer, C. Ambrosch-Draxl, and M. Scheffler, "Van der Waals interactions between organic adsorbates and at organic/inorganic interfaces," *MRS Bulletin* **35**, 435–442 (2010).
- ¹⁴W. Liu, A. Tkatchenko, and M. Scheffler, "Modeling adsorption and reactions of organic molecules at metal surfaces," *Accounts of Chemical Research* **47**, 3369–3377 (2014).
- ¹⁵M. Stöhr, T. Van Voorhis, and A. Tkatchenko, "Theory and practice of modeling van der Waals interactions in electronic-structure calculations," *Chemical Society Reviews* **48**, 4118–4154 (2019).
- ¹⁶D. Yuan, Y. Zhang, W. Ho, and R. Wu, "Effects of van der Waals Dispersion Interactions in Density Functional Studies of Adsorption, Catalysis, and Tribology on Metals," *The Journal of Physical Chemistry C* **124**, 16926–16942 (2020).
- ¹⁷P. Hohenberg and W. Kohn, "Inhomogeneous electron gas," *Physical Review* **136**, B864 (1964).
- ¹⁸W. Kohn and L. J. Sham, "Self-consistent equations including exchange and correlation effects," *Physical Review* **140**, A1133 (1965).
- ¹⁹R. O. Jones, "Density functional theory: Its origins, rise to prominence, and future," *Reviews of Modern Physics* **87**, 897 (2015).
- ²⁰J. P. Perdew and K. Schmidt, "Jacob's ladder of density functional approximations for the exchange-correlation energy," in *AIP Conference Proceedings*, Vol. 577 (American Institute of Physics, 2001) pp. 1–20.
- ²¹J. F. Dobson, J. Wang, B. P. Dinte, K. McLennan, and H. M. Le, "Soft cohesive forces," *International Journal of Quantum Chemistry* **101**, 579–598 (2005).
- ²²H.-V. Nguyen and G. Galli, "A first-principles study of weakly bound molecules using exact exchange and the random phase approximation," *The Journal of Chemical Physics* **132**, 044109 (2010).
- ²³M. Dion, H. Rydberg, E. Schröder, D. C. Langreth, and B. I. Lundqvist, "Van der Waals density functional for general geometries," *Physical Review Letters* **92**, 246401 (2004).
- ²⁴K. Lee, É. D. Murray, L. Kong, B. I. Lundqvist, and D. C. Langreth, "Higher-accuracy van der Waals density functional," *Physical Review B* **82**, 081101 (2010).
- ²⁵O. A. Vydrov and T. Van Voorhis, "Nonlocal van der Waals density functional: The simpler the better," *The Journal of Chemical Physics* **133**, 244103 (2010).
- ²⁶R. Sabatini, T. Gorni, and S. De Gironcoli, "Nonlocal van der Waals density functional made simple and efficient," *Physical Review B* **87**, 041108 (2013).
- ²⁷A. D. Becke and E. R. Johnson, "A density-functional model of the dispersion interaction," *The Journal of Chemical Physics* **123**, 154101 (2005).
- ²⁸E. R. Johnson and A. D. Becke, "A post-Hartree–Fock model of intermolecular interactions," *The Journal of Chemical Physics* **123**, 024101 (2005).
- ²⁹A. D. Becke and E. R. Johnson, "A unified density-functional treatment of dynamical, nondynamical, and dispersion correlations," *The Journal of Chemical Physics* **127**, 124108 (2007).
- ³⁰S. Grimme, "Accurate description of van der Waals complexes by density functional theory including empirical corrections," *Journal of Computational Chemistry* **25**, 1463–1473 (2004).
- ³¹S. Grimme, "Semiempirical GGA-type density functional constructed with a long-range dispersion correction," *Journal of Computational Chemistry* **27**, 1787–1799 (2006).
- ³²S. Grimme, J. Antony, S. Ehrlich, and H. Krieg, "A consistent and accurate ab initio parametrization of density functional dispersion correction (DFT-D) for the 94 elements H–Pu," *The Journal of Chemical Physics* **132**, 154104 (2010).
- ³³S. Grimme, S. Ehrlich, and L. Goerigk, "Effect of the damping function in dispersion corrected density functional theory," *Journal of Computational Chemistry* **32**, 1456–1465 (2011).
- ³⁴V. G. Ruiz, W. Liu, E. Zojer, M. Scheffler, and A. Tkatchenko, "Density-functional theory with screened van der Waals interactions for the modeling of hybrid inorganic-organic systems," *Physical Review Letters* **108**, 146103 (2012).

- ³⁵J. Klimeš and A. Michaelides, "Perspective: Advances and challenges in treating van der Waals dispersion forces in density functional theory," *The Journal of Chemical Physics* **137**, 120901 (2012).
- ³⁶S. Jenkins, "Aromatic adsorption on metals via first-principles density functional theory," *Proceedings of the Royal Society A: Mathematical, Physical and Engineering Sciences* **465**, 2949–2976 (2009).
- ³⁷J. P. Perdew, K. Burke, and M. Ernzerhof, "Generalized gradient approximation made simple," *Physical Review Letters* **77**, 3865–3868 (1996).
- ³⁸Y. Zhang and W. Yang, "Comment on "Generalized gradient approximation made simple"," *Physical Review Letters* **80**, 890 (1998).
- ³⁹J. P. Perdew, A. Ruzsinszky, G. I. Csonka, O. A. Vydrov, G. E. Scuseria, L. A. Constantin, X. Zhou, and K. Burke, "Restoring the density-gradient expansion for exchange in solids and surfaces," *Physical Review Letters* **100**, 136406 (2008).
- ⁴⁰J. Klimeš, D. R. Bowler, and A. Michaelides, "Chemical accuracy for the van der Waals density functional," *Journal of Physics: Condensed Matter* **22**, 022201 (2009).
- ⁴¹A. D. Becke, "Density functional calculations of molecular bond energies," *The Journal of Chemical Physics* **84**, 4524–4529 (1986).
- ⁴²A. D. Becke, "Density-functional exchange-energy approximation with correct asymptotic behavior," *Physical Review A* **38**, 3098 (1988).
- ⁴³A. Becke, "On the large-gradient behavior of the density functional exchange energy," *The Journal of Chemical Physics* **85**, 7184–7187 (1986).
- ⁴⁴H. Yildirim, T. Greber, and A. Kara, "Trends in adsorption characteristics of benzene on transition metal surfaces: Role of surface chemistry and van der Waals interactions," *The Journal of Physical Chemistry C* **117**, 20572–20583 (2013).
- ⁴⁵F. Maaß, Y. Jiang, W. Liu, A. Tkatchenko, and P. Tegeder, "Binding energies of benzene on coinage metal surfaces: Equal stability on different metals," *The Journal of Chemical Physics* **148**, 214703 (2018).
- ⁴⁶W. Liu, V. G. Ruiz, G.-X. Zhang, B. Santra, X. Ren, M. Scheffler, and A. Tkatchenko, "Structure and energetics of benzene adsorbed on transition-metal surfaces: density-functional theory with van der Waals interactions including collective substrate response," *New Journal of Physics* **15**, 053046 (2013).
- ⁴⁷H. Peng and J. P. Perdew, "Rehabilitation of the Perdew-Burke-Ernzerhof generalized gradient approximation for layered materials," *Physical Review B* **95**, 081105 (2017).
- ⁴⁸A. V. Terentjev, L. A. Constantin, and J. Pitarke, "Dispersion-corrected PBEsol exchange-correlation functional," *Physical Review B* **98**, 214108 (2018).
- ⁴⁹S. Adhikari, H. Tang, B. Neupane, A. Ruzsinszky, and G. I. Csonka, "Molecule-surface interaction from van der Waals-corrected semilocal density functionals: The example of thiophene on transition-metal surfaces," *Physical Review Materials* **4**, 025005 (2020).
- ⁵⁰J. Sun, A. Ruzsinszky, and J. P. Perdew, "Strongly Constrained and Appropriately Normed Semilocal Density Functional," *Physical Review Letters* **115**, 036402 (2015).
- ⁵¹E. B. Isaacs and C. Wolverton, "Performance of the strongly constrained and appropriately normed density functional for solid-state materials," *Physical Review Materials* **2**, 063801 (2018).
- ⁵²N. K. Nepal, S. Adhikari, J. E. Bates, and A. Ruzsinszky, "Treating different bonding situations: Revisiting Au-Cu alloys using the random phase approximation," *Physical Review B* **100**, 045135 (2019).
- ⁵³N. K. Nepal, S. Adhikari, B. Neupane, and A. Ruzsinszky, "Formation energy puzzle in intermetallic alloys: Random phase approximation fails to predict accurate formation energies," *Physical Review B* **102**, 205121 (2020).
- ⁵⁴Y. Fu and D. J. Singh, "Applicability of the strongly constrained and appropriately normed density functional to transition-metal magnetism," *Physical Review Letters* **121**, 207201 (2018).
- ⁵⁵J. Sun, R. C. Remsing, Y. Zhang, Z. Sun, A. Ruzsinszky, H. Peng, Z. Yang, A. Paul, U. Waghmare, X. Wu, *et al.*, "Accurate first-principles structures and energies of diversely bonded systems from an efficient density functional," *Nature Chemistry* **8**, 831 (2016).
- ⁵⁶C. Shahi, J. Sun, and J. P. Perdew, "Accurate critical pressures for structural phase transitions of group IV, III-V, and II-VI compounds from the SCAN density functional," *Physical Review B* **97**, 094111 (2018).
- ⁵⁷N. K. Nepal, A. Ruzsinszky, and J. E. Bates, "Rocksalt or cesium chloride: Investigating the relative stability of the cesium halide structures with random phase approximation based methods," *Physical Review B* **97**, 115140 (2018).
- ⁵⁸N. K. Nepal, L. Yu, Q. Yan, and A. Ruzsinszky, "First-principles study of mechanical and electronic properties of bent monolayer transition metal dichalcogenides," *Physical Review Materials* **3**, 073601 (2019).
- ⁵⁹J. Yu, G. Fiorin, H. Peng, M. L. Klein, and J. P. Perdew, "Different bonding type along each crystallographic axis: Computational study of poly (p-phenylene terephthalamide)," *Physical Review Materials* **4**, 055601 (2020).
- ⁶⁰P. D. Mezei, G. I. Csonka, and M. Kállay, "Simple modifications of the SCAN meta-generalized gradient approximation functional," *Journal of Chemical Theory and Computation* **14**, 2469–2479 (2018).
- ⁶¹H. Peng, Z.-H. Yang, J. P. Perdew, and J. Sun, "Versatile van der Waals density functional based on a meta-generalized gradient approximation," *Physical Review X* **6**, 041005 (2016).
- ⁶²S. Grimme, "Accurate description of van der Waals complexes by density functional theory including empirical corrections," *Journal of Computational Chemistry* **25**, 1463–1473 (2004).
- ⁶³S. Grimme, "Semiempirical GGA-type density functional constructed with a long-range dispersion correction," *Journal of Computational Chemistry* **27**, 1787–1799 (2006).
- ⁶⁴S. Grimme, J. Antony, S. Ehrlich, and H. Krieg, "A consistent and accurate ab initio parametrization of density functional dispersion correction (DFT-D) for the 94 elements H-Pu," *The Journal of Chemical Physics* **132**, 154104 (2010).
- ⁶⁵S. Grimme, S. Ehrlich, and L. Goerigk, "Effect of the damping function in dispersion corrected density functional theory," *Journal of Computational Chemistry* **32**, 1456–1465 (2011).
- ⁶⁶J. Tao, H. Tang, A. Patra, P. Bhattarai, and J. P. Perdew, "Modeling the physisorption of graphene on metals," *Physical Review B* **97**, 165403 (2018).
- ⁶⁷H. Tang, J. Tao, A. Ruzsinszky, and J. P. Perdew, "A van der Waals Correction to the Physisorption of Graphene on Metal Surfaces," *The Journal of Physical Chemistry C* (2019).
- ⁶⁸I. Lifshitz and A. Kosevich, "Theory of magnetic susceptibility in metals at low temperatures," *Soviet physics - JETP* **2**, 636–645 (1956).
- ⁶⁹E. Zaremba and W. Kohn, "Van der waals interaction between an atom and a solid surface," *Physical Review B* **13**, 2270 (1976).
- ⁷⁰E. Zaremba and W. Kohn, "Theory of helium adsorption on simple and noble-metal surfaces," *Physical Review B* **15**, 1769 (1977).
- ⁷¹X.-P. Jiang, F. Toigo, and M. W. Cole, "The dispersion force of physical adsorption: I. Local theory," *Surface Science* **145**, 281–293 (1984).
- ⁷²X.-P. Jiang, F. Toigo, and M. W. Cole, "The dispersion force of physical adsorption: II. Nonlocal theory," *Surface Science* **148**, 21–36 (1984).
- ⁷³P. Schwerdtfeger and J. K. Nagle, "2018 Table of static dipole polarizabilities of the neutral elements in the periodic table," *Molecular Physics* **117**, 1200–1225 (2019), <https://doi.org/10.1080/00268976.2018.1535143>.
- ⁷⁴NIST Computational Chemistry Comparison and Benchmark Database, NIST Standard Reference Database Number 101 Release 21, August 2020, Editor: Russell D. Johnson III, <http://cccbdb.nist.gov/>.
- ⁷⁵S. M. Smith, A. N. Markevitch, D. A. Romanov, X. Li, R. J. Levis, and H. B. Schlegel, "Static and dynamic polarizabilities of conjugated molecules and their cations," *The Journal of Physical Chemistry A* **108**, 11063–11072 (2004).
- ⁷⁶D. Delaere, M. T. Nguyen, and L. G. Vanquickenborne, "Influence of building block aromaticity in the determination of electronic properties of five-membered heterocyclic oligomers," *Physical Chemistry Chemical Physics* **4**, 1522–1530 (2002).
- ⁷⁷K. P. Withanage, S. Akter, C. Shahi, R. P. Joshi, C. Diaz, Y. Yamamoto, R. Zope, T. Baruah, J. P. Perdew, J. E. Peralta, *et al.*, "Self-interaction-free electric dipole polarizabilities for atoms and their ions using the Fermi-Löwdin self-interaction correction," *Physical Review A* **100**, 012505 (2019).
- ⁷⁸P. Hao, Y. Fang, J. Sun, G. I. Csonka, P. H. Philipsen, and J. P. Perdew, "Lattice constants from semilocal density functionals with zero-point phonon correction," *Physical Review B* **85**, 014111 (2012).
- ⁷⁹D. J. Carter and A. L. Rohl, "van der Waals corrected density functional calculations of the adsorption of benzene on the Cu (111) surface," *Journal of Computational Chemistry* **35**, 2263–2271 (2014).
- ⁸⁰A. H. Larsen and *et al.*, "The atomic simulation environment—a python library for working with atoms," *Journal of Physics: Condensed Matter*

- 29**, 273002 (2017).
- ⁸¹S. R. Bahn and K. W. Jacobsen, “An object-oriented scripting interface to a legacy electronic structure code,” *Comput. Sci. Eng.* **4**, 56–66 (2002).
- ⁸²W. R. Harshbarger and S. Bauer, “An electron diffraction study of the structure of thiophene, 2-chlorothiophene and 2-bromothiophene,” *Acta Crystallographica Section B: Structural Science, Crystal Engineering and Materials* **26**, 1010–1020 (1970).
- ⁸³D. Mootz and H.-G. Wussow, “Crystal structures of pyridine and pyridine trihydrate,” *The Journal of Chemical Physics* **75**, 1517–1522 (1981).
- ⁸⁴H. Tang, J. Tao, J. P. Perdew, *et al.*, “Density functionals combined with van der Waals corrections for graphene adsorbed on layered materials,” *Physical Review B* **101**, 195426 (2020).
- ⁸⁵J. Brandenburg, J. Bates, J. Sun, and J. Perdew, “Benchmark tests of a strongly constrained semilocal functional with a long-range dispersion correction,” *Physical Review B* **94**, 115144 (2016).
- ⁸⁶A. Bilić, J. R. Reimers, N. S. Hush, R. C. Hoft, and M. J. Ford, “Adsorption of benzene on copper, silver, and gold surfaces,” *Journal of Chemical Theory and Computation* **2**, 1093–1105 (2006).
- ⁸⁷M. Xi, M. X. Yang, S. K. Jo, B. E. Bent, and P. Stevens, “Benzene adsorption on Cu (111): Formation of a stable bilayer,” *The Journal of Chemical Physics* **101**, 9122–9131 (1994).
- ⁸⁸X.-L. Zhou, M. Castro, and J. White, “Interactions of UV photons and low energy electrons with chemisorbed benzene on Ag (111),” *Surface Science* **238**, 215–225 (1990).
- ⁸⁹D. Syomin, J. Kim, B. E. Koel, and G. B. Ellison, “Identification of adsorbed phenyl (C₆H₅) groups on metal surfaces: Electron-induced dissociation of benzene on Au (111),” *The Journal of Physical Chemistry B* **105**, 8387–8394 (2001).
- ⁹⁰P. Redhead, “Thermal desorption of gases,” *Vacuum* **12**, 203–211 (1962).
- ⁹¹D. A. King, “Thermal desorption from metal surfaces: A review,” *Surface Science* **47**, 384–402 (1975).
- ⁹²J. Carrasco, W. Liu, A. Michaelides, and A. Tkatchenko, “Insight into the description of van der Waals forces for benzene adsorption on transition metal (111) surfaces,” *The Journal of Chemical Physics* **140**, 084704 (2014).
- ⁹³Y. Jiang, S. Yang, S. Li, and W. Liu, “Aromatic molecules on low-index coinage metal surfaces: Many-body dispersion effects,” *Scientific Reports* **6**, 1–8 (2016).
- ⁹⁴S. T. u. R. Chowdhury, H. Tang, and J. P. Perdew, “van der Waals Corrected Density Functionals for Cylindrical Surfaces: Ammonia and Nitrogen Dioxide Adsorbed on a Single-Walled Carbon Nanotube,” in preparation (2021).
- ⁹⁵B. Hammer and J. Nørskov, “Electronic factors determining the reactivity of metal surfaces,” *Surface Science* **343**, 211–220 (1995).
- ⁹⁶B. Hammer and J. K. Nørskov, “Why gold is the noblest of all the metals,” *Nature* **376**, 238–240 (1995).
- ⁹⁷B. Hammer and J. K. Nørskov, “Theoretical surface science and catalysis—calculations and concepts,” *Advances in Catalysis* **45**, 71–129 (2000).
- ⁹⁸W. Liu, F. Maaß, M. Willenbockel, C. Bronner, M. Schulze, S. Soubatch, F. S. Tautz, P. Tegeder, and A. Tkatchenko, “Quantitative prediction of molecular adsorption: structure and binding of benzene on coinage metals,” *Physical Review Letters* **115**, 036104 (2015).
- ⁹⁹P. Milligan, B. Murphy, D. Lennon, B. Cowie, and M. Kadodwala, “A complete structural study of the coverage dependence of the bonding of thiophene on Cu (111),” *The Journal of Physical Chemistry B* **105**, 140–148 (2001).
- ¹⁰⁰G.-J. Su, H.-M. Zhang, L.-J. Wan, and C.-L. Bai, “Phase transition of thiophene molecules on Au (1 1 1) in solution,” *Surface Science* **531**, L363–L368 (2003).
- ¹⁰¹G. Rousseau, N. Bovet, S. Johnston, D. Lennon, V. Dhanak, and M. Kadodwala, “The structure of a coadsorbed layer of thiophene and CO on Cu (111),” *Surface Science* **511**, 190–202 (2002).
- ¹⁰²M. H. Dishner, J. C. Hemminger, and F. J. Feher, “Formation of a self-assembled monolayer by adsorption of thiophene on Au (111) and its photooxidation,” *Langmuir* **12**, 6176–6178 (1996).
- ¹⁰³P. Väterlein, M. Schmelzer, J. Taborski, T. Krause, F. Viczian, M. Bäßler, R. Fink, E. Umbach, and W. Wurth, “Orientation and bonding of thiophene and 2, 2'-bithiophene on Ag (111): a combined near edge extended X-ray absorption fine structure and $x\alpha$ scattered-wave study,” *Surface Science* **452**, 20–32 (2000).
- ¹⁰⁴K. Tonigold and A. Groß, “Adsorption of small aromatic molecules on the (111) surfaces of noble metals: A density functional theory study with semiempirical corrections for dispersion effects,” *The Journal of Chemical Physics* **132**, 224701 (2010).
- ¹⁰⁵R. J. Maurer, V. G. Ruiz, J. Camarillo-Cisneros, W. Liu, N. Ferri, K. Reuter, and A. Tkatchenko, “Adsorption structures and energetics of molecules on metal surfaces: Bridging experiment and theory,” *Progress in Surface Science* **91**, 72–100 (2016).
- ¹⁰⁶P. Milligan, J. McNamara, B. Murphy, B. Cowie, D. Lennon, and M. Kadodwala, “A NIXSW and NEXAFS investigation of thiophene on Cu (111),” *Surface Science* **412**, 166–173 (1998).
- ¹⁰⁷G. Liu, J. A. Rodriguez, J. Dvorak, J. Hrbek, and T. Jirsak, “Chemistry of sulfur-containing molecules on Au (111): thiophene, sulfur dioxide, and methanethiol adsorption,” *Surface Science* **505**, 295–307 (2002).
- ¹⁰⁸A. Imanishi, T. Yokoyama, Y. Kitajima, and T. Ohta, “Structural and electronic properties of adsorbed thiophene on Cu (111) studied by S K-edge x-ray absorption spectroscopy,” *Bulletin of the Chemical Society of Japan* **71**, 831–835 (1998).
- ¹⁰⁹G. Vidali, G. Ihm, H.-Y. Kim, and M. W. Cole, “Potentials of physical adsorption,” *Surface Science Reports* **12**, 135–181 (1991).
- ¹¹⁰R. Diehl, T. Seyller, M. Caragiu, G. Leatherman, N. Ferralis, K. Pussi, P. Kaukasoina, and M. Lindroos, “The adsorption sites of rare gases on metallic surfaces: a review,” *Journal of Physics: Condensed Matter* **16**, S2839 (2004).
- ¹¹¹V. G. Ruiz, W. Liu, and A. Tkatchenko, “Density-functional theory with screened van der Waals interactions applied to atomic and molecular adsorbates on close-packed and non-close-packed surfaces,” *Physical Review B* **93**, 035118 (2016).
- ¹¹²P. L. Silvestrelli and A. Ambrosetti, “van der Waals-corrected Density Functional Theory simulation of adsorption processes on noble-metal surfaces: Xe on Ag (111), Au (111), and Cu (111),” *Journal of Low Temperature Physics* **185**, 183–197 (2016).
- ¹¹³É. D. Murray, K. Lee, and D. C. Langreth, “Investigation of exchange energy density functional accuracy for interacting molecules,” *Journal of Chemical Theory and Computation* **5**, 2754–2762 (2009).
- ¹¹⁴J. P. Perdew and W. Yue, “Accurate and simple density functional for the electronic exchange energy: Generalized gradient approximation,” *Physical Review B* **33**, 8800 (1986).
- ¹¹⁵H. Tang, S. T. u. R. Chowdhury, and J. P. Perdew, “Revised SCAN+rVV10,” in preparation (2021).